Human Acetylcholinesterase Inhibitors: Electronic-Topological and Neural Network Approaches to the Structure-Activity Relationships Study

F. Kandemirli*, [1], M. Saraçoglu[2] and V. Kovalishyn[3]

[1]*Department of Chemistry, Kocaeli University, 41000, Kocaeli, Turkey*

[2]*Department of Chemistry, Erciyes University, 38039, Kayseri, Turkey*

[3]*Biomedical Department, Institute of Bioorganic & Petroleum Chemistry, 253660, Ukraine*

Abstract: The Electronic-Topological (ETM) and Neural Network methods were applied to the study of the "structure–acetylcholinesterase (AChE) inhibitor activity" relationships for a series of physostigmine and N-benzylpiperidine derivatives. Molecular fragments specific for active compounds and breaks of activity were calculated for human AChE by applying the ETM and Neural Network methods. Requirements necessary for a compound to be active were formulated; they are the result of detailed analysis of all compounds under study. A comparative study of the activity features found for human AChE was performed.

Keywords: Human AChE Inhibitors, Electronic Topological Method, Neural Network Method.

INTRODUCTION

Alzheimer's disease (AD), the most common cause of dementia in the elderly, is a chronic, slowly progressive neurodegenerative disorder with characteristic deterioration of intellectual capacity in various domains: learning and memory, language abilities, reading and writing, praxis, interaction with the environment. One of the few undisputed evidences in the neuropathology of the AD is the loss of cholinergic neurons occurring in different areas of the central nervous system, mainly the cerebral cortex and the hippocampus [1-5].

One promising therapeutic strategy for activating central cholinergic functions has been the use of inhibitors of acetylcholinesterase (AChE). This enzyme is responsible for the metabolic hydrolysis of acetylcholine. Tacrine, donepezil, and rivastigmine are acetylcholinesterase inhibitors that increase the levels of acetylcholine at the synapse by blocking the breakdown of the neurotransmitter [6].

Previous computational studies can be divided into three groups:

1. Approaches used to model ligand-receptor interaction through docking (molecular dynamics); these have been applied to only small series [7];
2. Quantitative structure-activity relationship (QSAR) studies that use either Comparative Molecular field analysis (CoMFA) or conventional 2D QSAR methods. Mainly, this methodology aims at the development of simple mathematical models that correlate changes in biological activity with variations in the structure of molecules. These variations are accounted for by parameters (experimentally determined or calculated) that relate to physico-chemical properties of the compounds. The QSARs of AChE inhibitors were reviewed recently [8-16];
3. Electronic-topological method (ETM), which is a structural approach designed for the investigation of structure-property relationships. In "structure-AChE inhibitor activity" [17] relationship studies had been performed for three series of N-benzylpiperidine derivatives by using the ETM. The results of the study show how the use of the ETM makes it possible to bypass the incompatibility problem as to the experimental data.

The present study that uses the ETM and Neural Network methods as well, aims at finding new AChE inhibitors that can be useful against AD.

MATERIALS AND METHODS

Data Sets

Compounds under study (73 molecules in total [18-22] are shown in Table **1**. Their common structural skeletons are given in (Fig. **1**). that shows how compounds under study belong to different structural classes. Skeletons **A, B** and **F** represent various derivatives of 4-(3-benzisoxazolylethyl)-N-benzylpiperidine. Molecular skeletons **C, D,** and **E** represent modifications performed on the structure of the natural product physostigmine.

Table **1** reports calculated and experimental log $1/IC_{50}$, measured on human erythrocyte AChE of 73 compounds. Molecules under study were classified as active compounds (31 molecules with log $1/IC_{50} \geq 7.24$), low-active ones (13 molecules with $7.22 \leq \log 1/IC_{50} \leq 6.81$) and inactive compounds (29 molecules with log $1/IC_{50} < 6.80$).

To identify activity features (or pharmacophores), the ETM-calculations were carried out twice: first, low-active compounds were considered as belonging to the active class, and then as belonging to the inactive class.

*Address correspondence to this author at the Department of Chemistry, Kocaeli University. Kocaeli, Turkey; Tel: +90 262 528 57 61; Fax: +90 262+3215968; E-mail: fkandemirli@yahoo.com

1389-5575/05 $50.00+.00

Table 1. ***In Vitro*** **Inhibition of Human AChE by Physostigmine and N-Benzylpiperidine Derivatives and Prognostigation of Activity**

No.	Skel-eton	X	R1	R2	log 1/IC$_{50}$		No	Skel-eton	X	R1	R2	log 1/IC$_{50}$	
					Exper	Theor						Exper	Theor
1	A		A1		9.48	8.27	38	D	*n*-C_4H_9	C_2H_5	CH_3	7,05	7.35
2	A		A2		9.32	8.30	39	D	*n*-C_7H_{15}	*n*-C_3H_7	CH_3	7,03	6.90
3	A		A3		9.24	8.26	40	B	6-CN			7,00	7.30
4	B	B1			9,10	8.30	41	F		$(CH_2)_2$	NH	6,97	7.20
5	A		A4		9,02	8.41	42	D	*n*-C_7H_{15}	CH_3	CH_3	6,94	7.30
6	B	6-$NHCOCH_3$			8,55	8.35	43	C	4-CH_3Ph	CH_3		6,86	6.75
7	A		A5		8,44	8.35	44	D	*n*-C_3H_7	C_2H_5	CH_3	6,81	6.92
8	B	5,6-$(CH_3)_2$			8,24	8.36	45	D	C_6H_5	C_2H_5	CH_3	6,75	6.82
9	B	7-OCH_3			8,15	8.36	46	D	*n*-C_6H_{13}	C_2H_5	H	6,68	5.82
10	B	5-OCH_3			8,14	8.37	47	F		$(CH_2)_2$	CH=CH	6,66	6.51
11	B	5-CH_3			8,11	8.34	48	D	CH_3	C_2H_5	H	6,60	6.45
12	B	6-OCH_3			8,08	8.38	49	C	C_8H_{17}	CH_3		6,54	6.52
13	B	6-$CONH_2$			8,06	8.37	50	C	4-*i*-C_3H_7Ph	H		6,49	6.39
14	B	6-$NHCOC_6H_5$			8,03	8.38	51	F		$NH\text{-}CH_2$	O	6,49	6.35
15	C	2-C_2H_5Ph	CH_3		8,01	8.11	52	F		$(CH_2)_2$	N=CH	6.47	6.29
16	C	2-CH_3Ph	CH_3		7,99	7.75	53	E	7			6,42	6.24
17	C	2,4-$(CH_3)_2$Ph	CH_3		7,87	7.85	54	D	*n*-C_7H_{15}	C_2H_5	H	6,42	6.23
18	C	Ph	H		7,86	7.64	55	C	2-ClPh	CH_3		6,31	6.32
19	B	6-$NHSO_2C_6H_5$			7,85	7.99	56	D	*n*-C_7H_{15}	$CH_2C_6H_5$	CH_3	6,30	5.87
20	C	2-*i*-C_3H_7Ph	CH_3		7,81	7.62	57	D	*n*-C_6H_{13}	*n*-C_3H_7	H	6,26	5.84
21	C	2-CH_3Ph	H		7,77	7.39	58	D	*n*-C_7H_{15}	*n*-C_3H_7	H	6,20	5.84
22	C	2,4-(CH_3)Ph	H		7,76	7.35	59	E	2			6,16	6.67
23	B	6-NH_2			7,70	7.81	60	C	4-*i*-C_3H_7Ph	CH_3		6,12	5.99
24	C	Ph	CH_3		7,62	8.38	61	F		$NH(CH_2)_2$	O	6.09	5.89
25	B	6-OH			7,59	7.30	62	F		$(CH_2)_3$	O	6.05	5.87
26	C	CH_3	CH_3		7,52	8.39	63	E	6			6,03	5.93
27	D	CH_3	C_2H_5	CH_3	7,42	7.20	64	D	*n*-C_4H_9	C_2H_5	H	5,97	5.89
28	D	*n*-C_6H_{13}	C_2H_5	CH_3	7,35	6.99	65	C	2,4,6-$(CH_3)_3$Ph	CH_3		5,89	5.79
29	B	6-Br			7,30	7.05	66	D	$CH(CH_3)C_6H_5$	C_2H_5	CH_3	5,88	5.90
30	B	H			7,26	7.02	67	C	2,6-$(C_2H_5)_2$4 -CH_3Ph	CH_3		5,83	5.84
31	D	*n*-C_7H_{15}	C_2H_5	CH_3	7,24	8.42	68	D	*n*-C_3H_7	C_2H_5	H	5,66	5.62
32	E	9			7,22	7.10	69	E	3			5,42	5.66
33	D	*n*-C_6H_{13}	*n*-C_3H_7	CH_3	7,21	7.12	70	E	5			5,12	5.99
34	C	2,6-$(Cl)_2$Ph	CH_3		7,18	6.90	71	F		O-CH_2	O	5.59	5.52
35	D	$CH_2C_6H_5$	C_2H_5	CH_3	7,16	7.40	72	D	*t*-C_4H_9	C_2H_5	CH_3	4,90	5.74
36	E	8			7,10	7.30	73	E	4			4,68	4.56
37	D	*n*-C_6H_{13}	CH_3	CH_3	7,11	7.35							

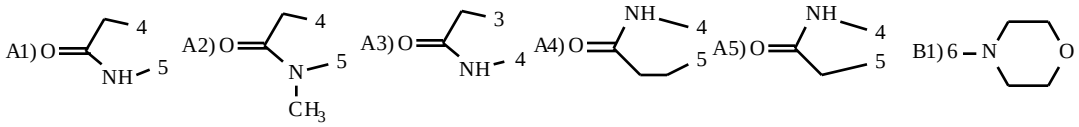

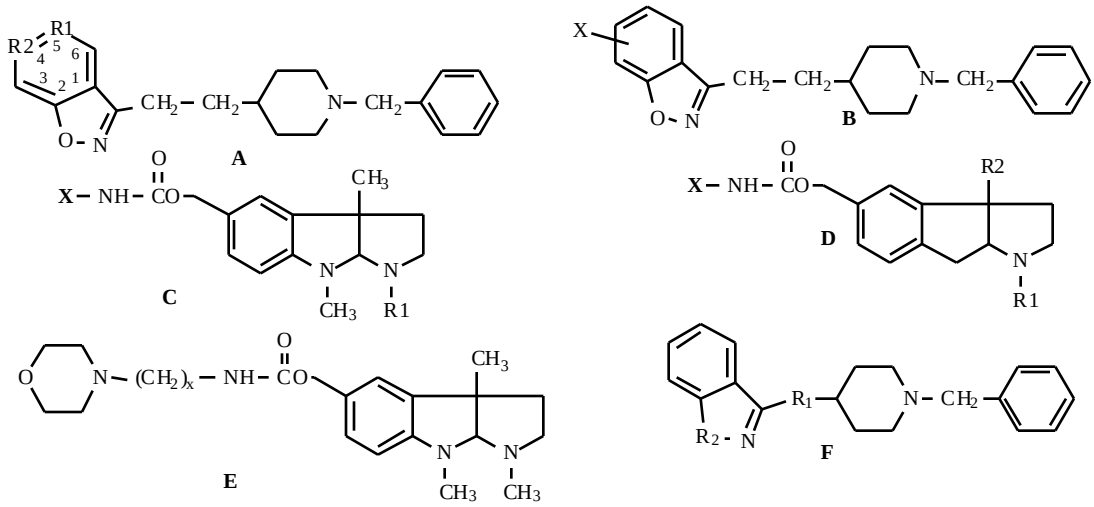

Fig. (1). Common molecular skeletons of the compounds under study.

ET Method Description

The ETM can be considered as one of structure-based approaches [23-26]. As all structural methods, it needs a language for the compounds structure description (LCSD). Because three-dimensional (3D) graphs are taken as models for real molecules, mathematical structures used in the ETM as LCSD are commonly used in QSAR matrices (one matrix = one compound). However, the nature of their elements is different. Instead of some global chemical properties (lipophilicity, solubility) used in QSAR methods, the ETM uses quantum-chemical, or electronic characteristics and data taken from conformational analysis. Conformational analysis and quantum chemistry calculations were carried out by means of molecular mechanics method (MMP2) and semi-empirical quantum chemistry method (AM1), respectively.

Diagonal elements of the matrices called Electronic-Topological Matrices of Contiguity (ETMC, for short) reflect one or more atomic properties (represented by a separate value or a vector of characteristics). Off-diagonal elements characterise bonds between pairs of atoms, if they exist, or distances, otherwise. (Usually, only the upper triangle of the matrix is used in calculations because of the symmetry of bonds.) Values of the bond properties can be also represented by one or more values. However, only one value is used in calculation for simplicity. If there are more than one properties for atoms and bonds, the ETM calculations can be repeated for every separate property. The formal description of the ETM can be found in [17].

Computational part of the ETM is a sequence of the following steps:

- Conformational analysis
- Quantum–chemical calculations
- ETMCs formation
- Processing ETMCs (the search of the structural features responsible for activity/inactivity by comparing a template active/inactive compound with the rest of compounds).

The last two steps represent the essential part of the ETM. The core of the ETM-software (see Fig. **2**) mainly follows a common scheme for the pattern recognition, but it has also some peculiarities that stem from complexity of the "structure-property" problem. A pattern recognition-based application consists of the following stages. The first stage is known as *data transforming*, when input data must be prepared in a predefined format. In the ETM-scheme, this stage serves for an ETMC formation for every molecule S^i.

The second stage, *pre-processing* (known also as *feature selection*) is to be done, aiming at the definition of common molecular fragments (i.e. congruent subgraphs S^j_A, j J; "A" means "responsible for the given activity"). They are searched for in *all* structures S^i, i I. A straightforward solution is to search them by comparing, one by one, molecular structures S^i with a *template* S^0 (an active compound, if features of activity are searched). Algorithms applied at this stage are named *self-learning* procedures. The corresponding algorithm of the ETM needs a number of initial parameters of the ETM algorithm. They are:

a) A threshold of activity, which allows the separation of all compounds into corresponding groups;

b) A template molecule for the comparison;

c) Values $\Delta_{1\text{-}3}$ that are used to fix a definite level of flexibility of molecules;

d) A desired value of a criterion $\boldsymbol{C_A}(S^j_A)$ (probability of a fragment S^j_A presence in the set $\{S^k_A\}$ of molecular structures).

The estimation of the probability for a S^j_A, is calculated by the following formula proved in structural methods:

$$\boldsymbol{C_A}\,(S^j_A) = (L_A+1)/(\,L_A + L_{NA} +2) \qquad (1)$$

Where L_A, L_{NA} are numbers of compounds from the $\{S^k_A\}$ and $\{S^k_{NA}\}$ sets, respectively, which contain the S^j_A fragment. If the fragments found satisfy the criterion C_A and are informative enough, from the point of view of the researcher, the procedure stops. Otherwise, it is repeated with different initial settings.

Next important stage in both indirect methods and some structural ones is an *examination procedure*. In the case of the ETM application, however, the found fragments can be

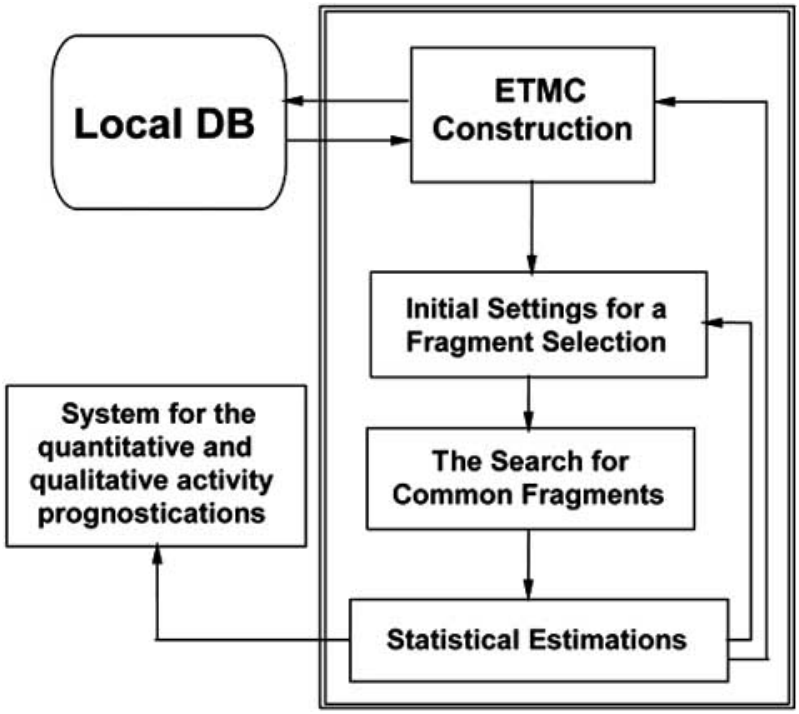

Fig. (2). Common scheme of ETM.

used immediately, if they satisfy some conditions superimposed by the researcher. At the same time, the examination procedure is applied when the researcher wants to validate the *stability* of the fragments selected. This is done by the "leave-one-alone" technique, when all compounds from the set $\{S^k_A\}$ are tried as templates for matrices' comparison. In contrast to many other methods in the ETM, this task is fulfilled by the same procedure as the one used at the previous step. The features validation is *obligatory*, when a quantitative (functional) model is to be developed on the basis of the fragments found (as usually is the case of indirect methods).

The concluding step is the development of a set of decision rules for the activity (A) prediction. In the ETM, this set is represented by a set of molecular substructures (represented by submatrices of ETMCs, or by ETSA, for short) and some numerical data that are important for recognising new molecular structures possessing the activity A. When having such set, the given property P prediction consists in the search of congruent subgraphs in all abovementioned structures S^i. Again, this procedure follows the same steps as the procedures for features selection and validation, but its initial settings $\Delta_{1\text{-}3}$ and $\boldsymbol{C_P}$ are those calculated at the first step, and templates are exactly the features selected.

When successfully found, a feature S^j_A elucidates core mechanisms of the receptor-ligand interactions. But a similar study can be carried out when the user wishes to find 'breaks of activity', which indirectly characterise sterically inaccessible and/or electronically forbidden regions of receptors. They are fragments that are common to all compounds from $\{S^l_{NA}$, for all $l\}$ and cannot be found in the compounds from $\{S^k_A$, for all $k\}$. (It is noteworthy that for a break of activity S^j_{NA} the criterion $\boldsymbol{C_{NA}}$ looks similar.) When used together, both types of features represent valuable information for the design of new compounds with the desired activity A.

NEURAL NETWORK METHOD

Artificial Neural Networks (ANNs) is a group of methods that are increasingly being used in drug design to study QSAR [27, 28]. This method is able to elucidate structure-activity relationships and take into account any non-linear character of these relationships. Thus, this method can be of significant interest in 3D QSAR studies.

For the analysis of the data we have used one of the most well-known neural networks - the feed forward neural networks (FFNNs) trained with the back propagation algorithm [29, 30]. The architecture of the ANNS was consisted of three-layers with five neurons in one hidden layer. One single output node was used to code activities of AChE inhibitors. The bias neuron was presented on the input and on the hidden layer. At least M=200 independent FFNN were trained to analyse each set of variables. The predicted values of each analysed case were averaged over all M network predictions and the means were used to calculate statistical coefficients with targets. The other details of the algorithm can be found elsewhere [31, 32].

The avoidance of overfitting/overtraining has been shown to be an important factor for the improvement of predictive ability and correct selection of variables in the feed forward neural networks [31]. The Early Stopping over Ensemble (ESE) technique was used in the current study to accomplish this. A detailed description of ESE can be found in [31, 32]. In brief, each analysed artificial neural network ensemble (ANNE) was composed of M=200 networks. The values calculated for analysed cases were averaged over all M neural

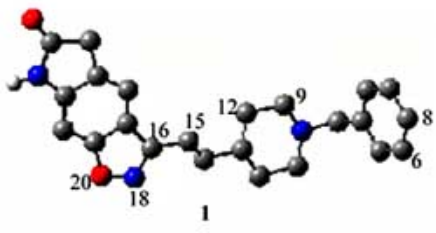

a

C_6	C_8	C_9	C_{12}	C_{15}	C_{16}	N_{18}	O_{20}
0.01	1.44	4.74	5.72	7.92	9.33	10.35	11.54
	0.00	5.17	6.29	8.78	10.20	11.13	12.38
		0.11	1.03	4.52	5.99	6.68	8.08
			0.00	3.07	4.52	5.18	6.58
				0.00	1.02	2.48	3.71
					0.13	1.76	2.25
					L_A/L_{NA}=19/0, C_A= *0.95*	-0.10	0.96
							-0.17

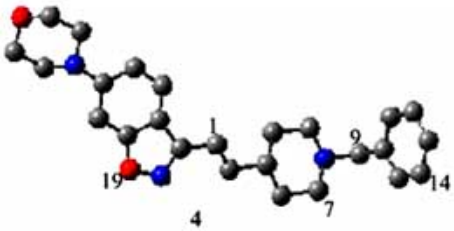

b

C_1	C_7	C_9	C_{14}	O_{19}
0.00	5.11	6.77	9.63	3.70
	0.11	2.42	4.53	8.16
		0.10	3.73	10.15
			0.02	12.53
			L_A/L_{NA}=22/0, C_A= *0.96*	-0.19

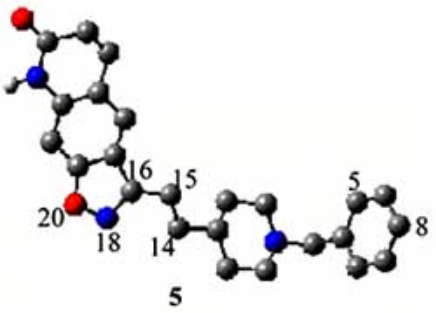

c

C_5	C_8	C_{14}	C_{15}	C_{16}	N_{18}	O_{20}
0.01	2.43	7.51	7.85	9.35	10.17	11.53
	0.00	8.78	8.71	10.14	11.09	12.34
		0.02	1.10	2.52	3.00	4.36
			0.00	1.02	2.47	3.71
				0.13	1.76	2.25
					-0.10	0.97
					L_A/L_{NA}=19/0, C_A= *0.95*	-0.17

Fig. (3). The **P1**(a), **P2**(b) and **P3**(c) pharmacophores found relative to active molecules **1, 4** and **5** respectively.

networks, and their means were used for computing statistical coefficients with targets. We used a subdivision of the initial training set into two equal learning/validation subsets. The first set was used to train the neural network while the second one was used to monitor the training process measured by root mean square error. An early stopping point determined as a best fit of a network to the validation set was used to stop the neural network learning. Thus, statistical parameters calculated at the early stopping point were used. The training was terminated by limiting the network run to 10, 000 epochs (total number of epochs) or after 2, 000 epochs (local number of epochs) following the last improvement of root–mean-square error in the early stopping point. The root–mean-square error *E* was computed as a criterion of network learning to determine the stop points of a training procedure. The quality of the model was tested by the leave-one-out cross-validation q^2 value defined as:

q^2 = *(SD-press)/SD;*

Introduced by Cramer *et al*. [33]. Here *SD* represents the variance of a target value relative to its mean and *'press'* is the average squared errors of predicted values obtained from leave-one-out (LOO) procedure.

The LOO cross-validation procedure was used to supervise the predictive performance of ANN.

It has been shown that pruning algorithms [34, 35] may be used to optimise the number of input parameters for ANNs learning and to select the most significant ones. These algorithms operate in a manner similar to step-wise multiple regression analysis and exclude on each step one input parameter that was estimated to be non-significant. The pruning algorithms were used in the current study to determine significant parameters of input data points of the analysed molecules as described in references [34, 35].

RESULTS AND DISCUSSION

According to the common scheme of the ETM, conformational analysis and quantum chemistry calculations were carried out for all compounds in the series under study. As the result of the conformational analysis, conformational structures with global minimum of their energies are to be found.

Pharmacophores and Anti-Pharmacophores Calculation

Electronic and steric parameters responsible for the activity form a matrix, which is a submatrix of the corresponding template ETMC. As it was already said, such submatrix is called the electron-topological submatrix of activity (ETSA). So, the activity feature (or pharmacophore) **P1** was calculated by taking molecule **1** as template compound ($\Delta_1 = \pm 0.05$, $\Delta_2 = \pm 0.10$). The **P1** is shown in (Fig. **3a**) along with its $ETSA_{P1}$.

The pharmacophore was found in 19 of 31 active compounds, and it was not found in inactive compounds at all. Thus, the probability C_A of its realisation in the active class is about 0.95. As seen from the pharmacophore's structure, it consists of the C_6, C_8 atoms of the phenyl, and C_9, C_{12}, C_{15}, C_{16}, N_{18}, O_{20} atoms.

Pharmacophore **P2** was calculated relative to the template molecule **4** in a similar way as for **P1** (see Fig. **3b**). The **P2** was found in 22 active compounds and it was not found in inactive compounds at all (correspondingly, the probability of its appearance is estimated as 0.96). The **P2** includes five atoms in total, as seen from (Fig. **3b**).

Pharmacophore **P3** was calculated by taking compound **5** as the template for comparison. The **P3** includes seven atoms, which are carbon atoms C_5, C_8, of the phenyl cycle and two carbons, C_{14}, C_{15}, C_{16}, N_{18}, O_{20}. They belong to different parts of the template molecule, and, as seen from (Fig. **3c**), they represent the most important two parts of all active molecules.

In Figure **4**, the superimposition of three template compounds that correspond to the calculated pharmacophores P1 – P3 is shown. In 3D space three separate regions can be indicated for each active molecule, where atoms of the three pharmacophores can be found.

These regions are shown in the (Fig. **4**) by dotted lines. One of them is formed by the atoms belonging to the phenyl ring, while the other two are formed by the atoms that represent the heterocyclic rings. It is quite possible that the atoms from these regions play an important role in the ligand-receptor interaction.

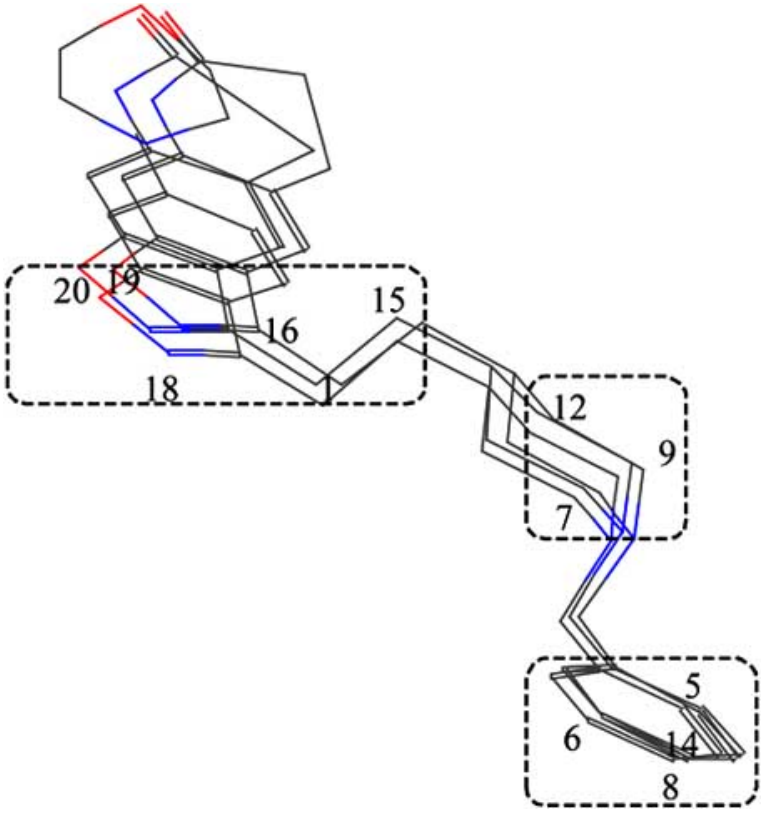

Fig. (4). Template compounds **1, 4** and **5** alignment by superposing the **P1, P2** and **P3** features.

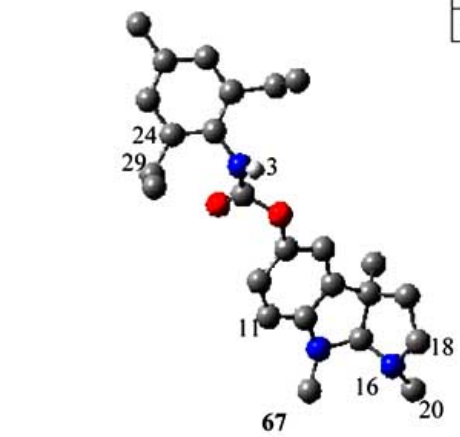

a

H_3	C_{11}	N_{16}	C_{18}	C_{20}	C_{24}	C_{29}
0.11	3.53	7.71	8.13	8.80	2.69	2.81
	-0.03	4.88	5.61	5.66	5.68	4.86
		-0.16	0.98	1.03	10.27	9.68
			0.10	2.45	10.75	10.28
				0.09	11.25	10.51
					0.02	1.01
						0.03

L_A/L_{NA}=2/21, C_A= *0.88*

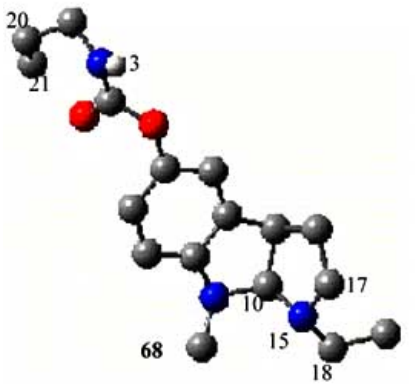

b

H_3	C_{10}	N_{15}	C_{17}	C_{18}	C_{20}	C_{21}
0.12	4.21	7.63	7.90	8.00	2.75	4.18
	0.02	3.68	4.33	4.26	6.52	8.00
		-0.17	0.99	1.00	10.12	11.57
			0.10	2.46	10.54	12.00
				0.0912	10.43	11.80
					0.01	1.04
						-0.00

L_A/L_{NA}=2/18, C_A= *0.86*

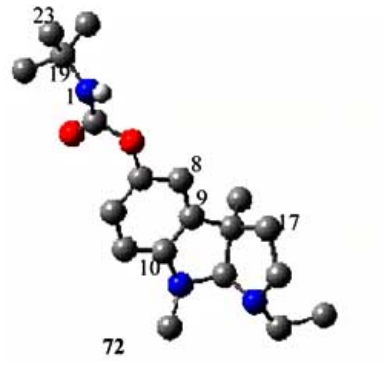

c

N_1	C_8	C_9	C_{10}	C_{17}	C_{19}	C_{23}
-0.22	3.85	4.76	4.90	8.45	0.95	2.49
	-0.05	1.45	2.34	4.74	5.28	6.21
		0.05	1.36	3.76	6.14	7.10
			0.00	4.33	6.16	7.00
				0.10	9.80	10.84
					0.17	1.00
						-0.03

L_A/L_{NA}=2/18, C_A= *0.86*

Fig. (5). The **AP1**(a), **AP2**(b) and **AP3**(c) anti-pharmacophore found relative to inactive molecules **67, 68** and **72** respectively.

When building a system for the activity prediction, those fragments of molecule are also to be taken into account, which are capable of deactivating an active structure ('breaks of activity', or anti-pharmacophores). An anti-pharmacophore **AP1** was found from template compound **67** (see Fig. **5a**). **AP1** contains seven atoms belonging to different parts of the template molecule **67**. These atoms are C_3, C_{11} C_{16}, C_{18}, C_{20}, C_{24} and C_{29}. Peculiarities of electronic-topological parameters such as atomic charges, bond multiplicities and interatomic 3D distances for the atoms can be seen from its $ETSC_{AP1}$. 3D distances used at place of some off-diagonal elements in the $ETSA_{AP1}$ are close enough. **AP1** feature was found in 21of 29 inactive compounds. It was found 2 in active compounds. So, the probability of its realisation (C_{NA}) in this class of compounds is about 0.88.

Anti-pharmacophore **AP2** was calculated from the template compound **68**. The atoms C_3, C_{10}, C_{15}, C_{17}, C_{18},

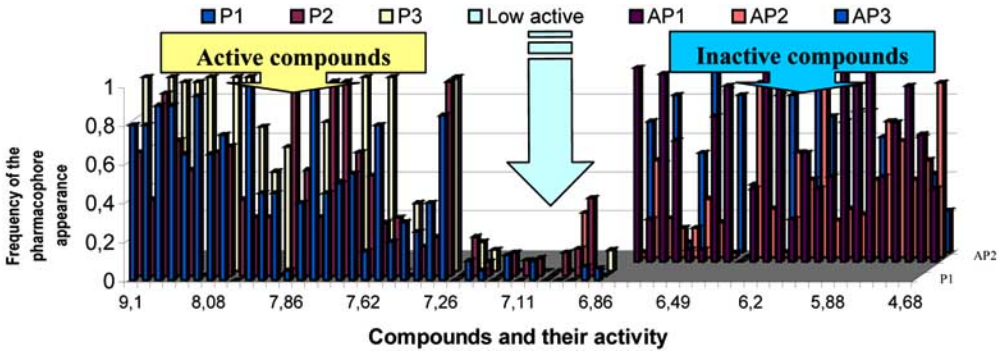

Fig. (6). Frequency of the fragments' occurrence in the compounds from the studied series for pharmacophores **P1** ÷ **P3** and for anti-pharmacophores **AP1** ÷ **AP3.**

$C_{20,}$ and C_{21} depicted in (Fig. **5b**) were found incapable of hydrogen bonds formation with the receptor. The **AP2** was found in 18 of 29 inactive compounds and 2 active compounds. Thus, the probability of its realisation was calculated as 0.86.

From the compound **73** taken as the template, the anti-pharmacophore **AP3** was calculated. The activity feature was found in 18 inactive compounds and in two of active compounds. As seen from (Fig. **5c**), **AP3** includes 7 atoms. The probability of its realisation in inactive compounds is equal to 0.86. Molecules become inactive ones H replaces methyl group in the R2 position to the **D** skeleton (see molecules **46, 48, 54, 56, 58, 64, 68** in Table **1**).

A para-substituted phenyl decreases the inhibiting activity of the compounds with skeleton **C** (compare compounds **16**, **43**, and also compounds **20**, **60**). Elongation of the substituents attached to nitrogen atoms (compare molecules **28**, **31**, **38** and **44)** causes the increase of inhibitory activity. The lengths of the chains of groups attached to molecules **44**, **38**, **28**, **31** grow respectively. Activity increases up to certain chain length (compounds **44**, **38**, **28**) and then decreases with the further growth of the chain length (**27, 31**). The same situation was observed in the series of molecules **68**, **64**, **46** and **54** (Skeleton D).

The ability of the aforementioned system to divide compounds of the training set into classes of activity/inactivity is illustrated in (Fig. **6**) by frequencies of the fragments occurrence in the compounds of the training set. The frequencies are shown in dependence with the level of AChE inhibition activity of the compounds in view.

As seen from the graph in the (Fig. **6**), in the class of active compounds there is a group of high- active compounds and another group of compounds of moderate activity. The value of log 1/IC50 ~ 7, 22-6.81 serves as a boundary between the two groups.

Neural Network Studies

15 pharmacophores and 15 anti-pharmacophores descriptors were used as parameters for the analysis with ANNs. The performance of neural networks was evaluated by LOO statistical coefficients calculated at early stopping point for the training data set. The high cross-validation value q^2 = 0.78±0.01 confirms the validity of the model for predicting activity of AChE inhibitors. At the second stage of analyses we decided to examine, if all 30 descriptors attributes are relevant for the prediction of activity AChE inhibitors. Application of pruning methods allowed to select only nine

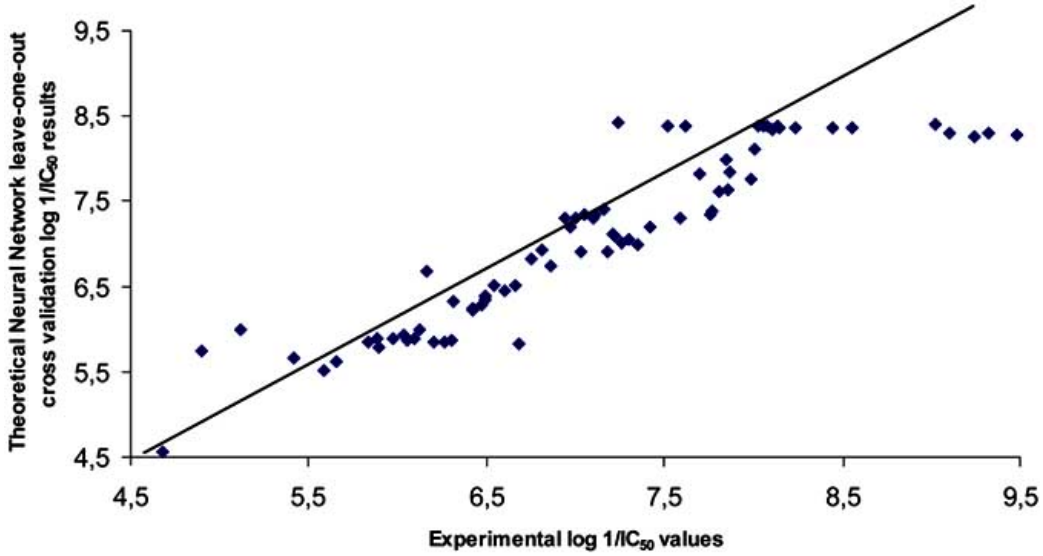

Fig. (7). Neural network leave-one-out cross validation log 1/IC50 results.

most relevant parameters (P1-P4, P11, P12, AP1-AP4, AP6, AP10) responsible for AChE inhibitor activities. The calculated result shows that the cross-validation value q^2= 0.81±0.01 as illustrated in (Fig. **7**), a strong linear dependency was obtained between the corresponding predicted and experimental values of the AChE inhibitor activities.

This result confirms our hypothesis that pharmacophore and anti-pharmacophore parameters obtained from ETM method can be used for coding each molecule and building QSAR model.

CONCLUSION

Early research aimed at the development of quantitative models for the structure-activity relationships in several series of AChE inhibitors have shown the importance of physical-chemical properties involved in the inhibitory activity [15]. As it follows from them, hydrophobicity, electronic and steric factors play a primary role in the equations found as the result of that work. However the resulting equations have low values of correlation coefficients and are hardly appropriate for inhibitory activity prognostication.

Systematic study was carried out by the ETM application in a series of compounds that are capable of demonstrating AChE inhibitory activity. Data obtained from conformation and quantum chemistry calculations were used to form electron-topological matrices. These matrices were effectively used to search for pharmacophores and anti-pharmacophores. In Table **1** the results of the theoretical prognosis of the human AChE inhibitory activity are given. As follows from the Table, the system of three pharmacophores and three anti-pharmacophores effectively separates compounds of the teaching set into groups of active and inactive compounds. Low-active molecules are badly responsive to the activity prognostication because they form a buffer zone consisting of compounds that can include both pharmacophores and anti-pharmacophores. The system is supposed to be applied to screening and design of new active compounds possessing skeletons similar to those used in the present study.

ACKNOWLEDGEMENTS

The authors thank Dr. N. Shvets for her assistance in carrying out the study.

REFERENCES

[1] Davidsson, P.; Blennow, K.; Andreasen, N.; Eriksson, B.; Minthon, L.; Hesse, C. *Neuroscience Letter*, **2001**, *300*, 157.
[2] Snape, M.F.; Misra, A.; Murray, T.K.; De Souza, R.J.; Williams, J.L.; Cross, A.J.; Green, A.R. *Neuropharmacology*, **1999**, *38*(1), 181.
[3] Shadlen, M.F.; Larson, B. *Postgraduate Med.*, **1999**, *105*(1), 109.
[4] Benzi, G.; Moretti, A. *Eur. J. Pharm*., **1998**, *346*(1), 1.
[5] Hasegawa, K. *Neurobiology of Aging*, **1998**, *19*, 107.
[6] Obata, R.; Sunazuka T.; Otoguro, K.; Tomoda, H.; Harigaya, Y.; Omura, S. *Bioorg. and Med. Chem. Letters*, **2000**, *10*, 1315.
[7] Yamamoto, Y.; Ishihara, Y.; Kuntz, I.D. *J. Med. Chem*., **1994**, *37*, 3141.
[8] Rampa, A.; Bisi, A.; Valenti, P.; Recanatini, M.; Cavalli, A.; Andrisano, V.; Cavrini, V.; Fin, L.; Buriani, A.; Giusti, P. *J. Med. Chem.*, **1998**, *41*, 3976.
[9] Fukutu, T.R.; Metcalf, R.L. *J. Agric. Food Chem.*, **1956**, *4*, 930.
[10] Hansch, C. *Accounts Chem. Res.*, **1993**, *26*, 147.
[11] Hansch, C.; Leo, A. Exploring QSAR. Fundamentals and Applications in Chemistry and Biology. American Chem. Society., **1995**, Washington. DC, pp. 169.
[12] Hansch, C. Materials and Pharmaceuticals, ACS Symposium Series 589, American Chem. Society., **1995**, Washigton. DC, pp. 281.
[13] Gupta, S.P. *Chem. Rev.*, **1987**, *87*, 1183.
[14] Magee, P.S. Chemicals Affecting Insects and Mites, in J.G. Topliss (Ed.), Quantitative Structure Activity Relationships of Drugs, New York, **1983**.
[15] Recanatini, M.; Cavalli, A.; Hansch, C. *Chem.-Biol. Interactions*, **1997**, *105*, 199.
[16] Tong, W.; Collantes, E.R.; Chen, Y.; Welsh, W.J. *J. Med. Chem.*, **1996**, *39*, 380.
[17] Dimoglo, A.S.; Shvets, N.M.; Tetko, I.V.; Livingstone, D.J. *Quant. Struct.-Act. Relat.*, **2001**, *20*, 31.
[18] Alisi, M.A.; Brufani, M.; Filicamo, L.; Gostoli, G.; Licandro, E.; Cesta, M.C.; Lappa, S.; Marchesini, D.; Pagella, P. *Bioorg. Med. Chem. Lett.*, **1995**, *5*, 2077.
[19] Brzostowska, M.; He, X.; Greig, N.H.; Rapoport, S.I.; Brossi, A. *J. Med. Chem. Res.*, **1992**, *2*, 238.
[20] Chen, Y.L.; Nielsen, J.; Hedberg, K.; Dunaiskis, A.; Jones, S.; Russo, L.; Johnson, J.; Ives, J.; Liston, D. *J. Med. Chem*., **1992**, *35*, 1429.
[21] Villalobos, A.; Blake, J.F.; Biggers, C.K.; Butler, T.W.; Chapin, D.S.; Chen, Y.L.; Ives, J.L.; Jones, S.B.; Liston, D.R.; Nagel, A.A.; Nason, D.M.; Nielsen, J.A.; Shalaby, I.A.; Frost, W. *J. Med. Chem.*, **1994**, *37*, 2721.
[22] Villalobos, A.; Butler, T.W.; Chapin, D.S.; Chen, Y.L.; DeMattos, S.B.; Ives, J.L.; Liston, D.R.; Nagel, A.A.; Nason, D.M.; Nielsen, J.A.; Ramires, A.D.; Shalaby, I.A.; Frost, W. *J. Med. Chem.*, **1995**, *38*, 2802.
[23] Dimoglo, A.S. *Khimiko-pharm. Zhurnal*, **1985**, (Rus) *4*, 438.
[24] Shvets, N.M. *Comp. Sci. J. Moldova*, **1993**, *1*, 101.
[25] Shvets, N.M. *Comp. Sci. J. Moldova*, **1997**, *3*, 301.
[26] Dimoglo, A.S.; Vlad, P.F.; Shvets, N.M.; Koltsa, M.N. *New J. Chem.*, **2001**, *25*, 283.
[27] Kovesdi, I.; Dominguez-Rodrigue, M.F.; Orfi, L.; Naray-Szabo, G.; Varro, A.; Papp, J.G.; Matyus, P. *Med. Res. Rev.*, **1999**, *19*, 249-269.
[28] Manallack, D.T.; Livingstone, D.J. *Eur. J. Med. Chem.*, **1999**, *34*, 195.
[29] Rumelhart, D.E.; Hinton, G.E.; Williams, R.J. Learning internal representations by error propagation. In Parallel Distributed Processing: Explorations in the Microstructure of Cognition, Rumelhart, D.E.; McClelland, J.L.; Eds. M.A., The MIT Press, Cambridge, **1986**.
[30] Zupan, J.; Gasteiger, J. Neural Networks for Chemistry and Drug Design: An Introduction, 2nd edition, VCH: Weinheim, **1999**.
[31] Tetko, I.V.; Livingstone, D.J.; Luik, A.I. *J. Chem. Inf. Comput. Sci.*, **1995**, *35*, 826.
[32] Tetko, I.V.; Villa, A.E.P. *Neural Networks*, **1997**, *10*, 1361.
[33] This coefficient was introduced as r^2 in Cramer RD III, Patterson, D.E.; Bunce, J.D. *J. Am. Chem. Soc.*, **1988**, 110, 5959-5967. However, in order to avoid confusion with the analogous conventional $r^2=R*R$ value the new designation q^2 was recommended in Cramer III RD, De Priest, S.A.; Patterson, D.E.; Hecht, P. *The Developing Practice of Comparative Field Analysis, In: 3D QSAR in Drug Design: Theory Methods and Applications*, **1993**, H. Kubinyi Ed, ESCOM, The Netherlands, pp. 443-486.
[34] Tetko, I.V.; Villa, A.E.P.; Livingstone, D.J. *J. Chem. Inf. Comput. Sci.*, **1996**, *36*, 794.
[35] Kovalishyn, V.V.; Tetko, I.V.; Luik, A.I.; Kholodovych, V.V.; Villa, A.E.P.; Livingstone, D.J. *J. Chem. Inf. Comput. Sci.*, **1998**, 38, 651.